Calculated Auger yields and sensitivity factors for *KLL–NOO* transitions with 1–10 kV primary beams

Susan Mroczkowski
Midwest Research Microscopy, Inc., Milwaukee, Wisconsin 53218

David Lichtman
Physics Department and Surface Studies Laboratory, University of Wisconsin at Milwaukee, Milwaukee, Wisconsin 53201

(Received 27 July 1984; accepted 20 February 1985)

Relative values of the calculated Auger yields for the major *KLL*, *LMM*, *MNN*, and *NOO* transitions are listed for those transitions initiated by 1, 3, 5, and 10 kV primary electron beams. Additionally, these values are normalized to sensitivity factors in the *Handbook of Auger Electron Spectroscopy* for the specific transitions and primary voltages. The calculated yields can be used for quantitation if the Auger spectra were collected in the $N(E)$ mode; the yields which have been normalized to *Handbook* values attempt to account for different derivative peak shapes and can be used for quantitation if the Auger spectra were collected in the $dN(E)/dE$ mode. A discussion of the assumptions used in the calculated values outlines the cases in which care must be used. Internal calibration is recommended for accurate quantitation of transitions with an energy less than 200 eV.

I. INTRODUCTION

When insulating samples are analyzed with Auger electron spectroscopy, the use of lower primary electron energies often alleviates charging problems. At the lower primary voltages, the only detectable peak for high atomic number elements is often that due to an *NOO* transition. Sensitivity factors for *NOO* transitions and for transitions caused by a 1 kV primary beam are not readily available, making accurate quantitative data difficult to obtain. In addition, the trend in current Auger data acquisition is towards collecting with pulse counting electronics rather than differentiated spectra collected with a lock-in amplifier. The reason for this trend, despite difficulties encountered with the large background, is due in part to the need to obtain more accurate quantitative data; the area under the curve is determined rather than measuring peak-to-peak height values. Sensitivity factors for the nondifferentiated spectra are also not readily available.

Calculated sensitivity factors have been shown to be a viable alternative to experimentally determined values. Earlier publications[1,2] showed that when conductive, high purity standards were available, calculated and experimental sensitivity factors correlate well. There is a considerable difference, sometimes an order of magnitude, when high purity standards are not available as in the light element and lanthanide series. In this report, the relative yields for the major *KLL*, *LMM*, *MNN*, and *NOO* transitions will be calculated for 1, 3, 5, and 10 kV primary electron beams. With an understanding of the assumptions in the calculated values, these yields can be used as sensitivity factors for nondifferentiated spectra because measuring the area under the curve accounts for peak-shape changes. The calculated yields are then normalized to the sensitivity factors in the *Handbook of Auger Electron Spectroscopy*[3] for use in quantitation of data collected in the derivative mode. The yields which have been normalized to the data in the *Handbook* have a different normalization factor for each of the four primary voltages and the four transition groups analyzed to account for changes in the peak shape across the periodic table. (Although the normalized yields have previously been graphically reported[2] for the *KLL*, *LMM*, and *MNN* transitions for 3, 5, and 10 kV, they are included in Table I for completeness.)

II. CALCULATION OF RELATIVE AUGER YIELD

The Auger electron current I_i for the *UVW* Auger transition of the ith element can be expressed as[1,2]:

$$I_i(UVW) = I_p\rho(UVW)T\sigma(E_p,E_c)RN_i(\chi_i)\lambda_i(\chi_i)r_i(E_p,\chi_i)\chi_i, \quad (1)$$

where I_p is the primary electron current, $\rho(UVW)$ is the *UVW* Auger transition probability, T the instrument response function, $\sigma(E_p,E_c)$ the ionization cross section which is a function of the primary energy E_p and the critical energy for ionization E_c, R a surface roughness factor, N_i the elemental atomic density, λ_i the elemental electron escape depth,[5] r_i the electron backscatter coefficient, and χ_i the atom fraction of the ith component in the volume analyzed.

The mathematical equations to determine the values for each of the components in Eq. (1) have been published previously.[1,2] Rather than reiterate the equations, the assumptions of each component will be discussed so that there will be an understanding of the possible shortcomings from the use of calculated sensitivity factors to obtain quantitative information.

Under constant instrumental conditions, such as angle of acceptance, etc., the Auger electron current of Eq. (1) can vary by over three orders of magnitude for pure elements. The factor which is most responsible for the overall range of the Auger electron yield is the ionization cross section. The equation of Gerlach and DuCharme[4] was used to calculate the ionization cross section. Their calculations for *K*-, *L*-,

 0734-2101/85/041860-06$01.00

and M-shell transitions were extended to N-shell transitions for this study. The cross section values were not adjusted for the effect of Coster–Kronig transitions. Previous calculations showed the Coster–Kronig transition-adjusted cross section ratios were changed by less than 2% even for corrections of a copper/gold binary series. This 2% is well within expected errors of other parameters. For a given Auger transition and primary energy, σ smoothly decreases with atomic number Z. The theory of Gerlach and DuCharme[4] assumes that the cross section is maximum when the energy of the primary beam E_p is four times the critical energy of ionization E_c. The reduced energy U is defined as E_p/E_c. As U approaches one, the cross section, and therefore the Auger yield, approaches zero. As U increases past four, there is a gradual decrease in the cross section and the yield. A plot of calculated σ versus U is shown in Fig. 1. Similar plots have been published elsewhere for both theoretical and experimental data.[11,13–15]

Variations in the atomic density factor N play a large part in determining the Auger yield of an element. Atomic density varies by an order of magnitude and is responsible for minima and maxima present in a plot of Auger yield versus atomic number.[2] Because the electron escape depth λ is an inverse function of N, the role of the atomic density gains more importance. As an example, the density of diamond is 176 atoms/nm^3 compared to 113 atoms/nm^3 for graphite. The corresponding difference in yield is a factor of 0.64. Clearly, quantitation of samples containing carbon as an adsorbed hydrocarbon should have some other density factor which may not be simple to determine.

The backscattering factor and the Auger transition probability vary slowly with atomic number over a small total range and their effect on the Auger electron yield is small.[2,6,7] For the transitions tabulated in this paper, the backscattering factors are generally in the range from 1.0–2.0 and the Auger transition probability varies from 0.92–1.00.

The sample roughness factor R will be assumed constant. Numerous papers[8,9] have been published discussing the lower signal obtained from rougher samples, but mathematical models which have been developed are somewhat uncertain and difficult to apply. This unquantifiable roughness factor is probably one of the major reasons why empirically determined sensitivity factors of sputtered metallic samples do not correlate to calculated values. The role of sample roughness in decreasing signal should not be taken lightly because roughness can decrease the AES signal of a pure element standard by a factor of 2.[8] As a comparison, although the backscattering factor varies by a factor of 2 across the entire Periodic Table, it only varies by at most 20% for a given element in another matrix.

The instrument response function T includes the multiplier response. It is assumed that the collection efficiency is constant for all Auger peaks above 200 eV, the approximate energy above which the electron multiplier gain is roughly constant. For transitions with energy less than 200 eV, caution must be used. The low multiplier gain at low energies is used to decrease the large secondary signal; it also decreases the peak-to-peak height of Auger transitions in that range, so the calculated values must be adjusted accordingly. This can vary from system to system, so internal calibrations should be done for each system.

With these assumptions, the Auger yield, defined as the fraction of generated Auger current out of the total primary electron current, is given in Eq. (2) for a pure element i:

$$I_i(UVW)/I_p \propto \rho(UVW)\sigma(E_p,E_c)N_i\lambda_i r_i(E_p,E_c). \quad (2)$$

McGuire[10] plots experimental yield versus primary energy ($E_p = 1.5 - 5.0$ kV in 500 V increments) for some elements. McGuire's data do not correlate to theory because the maximum yield does not always occur at $U = 4$. As the energy of the Auger peak decreases, the U of maximum yield increases. The maximum yield for sulfur LMM (150 eV) was found at $U = 21$; the maximum yield for nitrogen KLL (381 eV) was found at $U = 8$; the maximum yield for titanium LMM (417 eV) was found at $U = 6$. As E_x (the energy of the Auger electron) increased, the U of maximum yield approached four, as theory predicts. Smith and Gallon[11] plot yield versus reduced energy for carbon and find that it peaks at approximately $U = 4$. Their data for silicon (100 eV) and selenium (164 eV) maximize at about $U = 6$. The gadolinium peak at 111 eV maximizes at $U = 12$ and the gold peak at 87 eV maximizes at $U = 20$. These data of Smith and Gallon follow the same trend as McGuire's data.

This enhanced yield may be due to the energy distribution of the secondary electrons. The lower energy Auger transitions can occur with secondary electron excitation; as the energy of the Auger transition E_x increases, fewer secondaries have enough energy to cause the transition. Thus, the secondary electron contribution tends to become less significant for energies greater than about 200 eV. The increased yield at lower Auger electron energies is not expected to interfere greatly with the calculated yields from Eq. (2) if internal calibrations are run, i.e., if proper proportionality values are obtained for Auger electron energies below 200 eV. Powell[12] has completed first principles calculations similar to those outlined here. He compared measured and computed relative yields of LVV and KLL Auger electrons from aluminum for a 2 kV primary beam. The computed LVV/KLL intensity ratio was 13.7; the measured LVV/KLL intensity ratio was 12.6. This fairly good agreement was obtained without a correction for secondary electron energy distribution. His data were taken in the $N(E)$ mode.

III. THE USE OF RELATIVE YIELDS WITH NONDIFFERENTIATED SPECTRA

Table I lists relative values of the calculated Auger yield for primary electron beams of 1, 3, 5, and 10 kV for the major KLL, LMM, MNN, and NOO transitions. These yields can be used for quantitative information if the Auger data are collected in pulse counting mode. With this method, the Auger current is assumed to be proportional to the area under the peak.

Although accurate background subtraction is still a large limitation of this technique, this method is likely to be the more accurate because the area under the peak is a better measure of Auger current than the peak-to-peak heights used in derivative spectra. Care should be taken with peaks

TABLE I. Calculated relative Auger yields and sensitivity factors for *KLL*, *LMM*, *MNN*, and *NOO* transitions with 1, 3, 5, and 10 kV primary electron beams. The relative yield values should be used for quantitative AES data if the spectra were collected in the $N(E)$ mode. The normalized sensitivity factors attempt to account for derivative peak shapes and should be used for quantitative AES data if the spectra were collected in the $dN(E)/dE$ mode.

				Relative yield, $\rho\sigma N\lambda r \times 10^{20}$				Normalized sensitivity factor			
Element	Z	Transition	E_x(eV)	1 kV	3 kV	5 kV	10 kV	1 kV	3 kV	5 kV	10 kV
Li	3	*KLL*	43	16.8	7.02	4.5	2.5	6.3	2.8	1.8	1.05
Be	4	*KLL*	104	9.04	4.3	2.8	1.6	3.4	1.7	1.1	0.67
B	5	*KLL*	179	5.4	3.04	2.08	1.2	2.01	1.2	0.83	0.50
C(dia)	6	*KLL*	272	3.6	2.6	1.8	1.07	1.3[a]	1.04	0.73	0.46
N	7	*KLL*	379	0.84	0.83	0.62	0.38	0.31	0.33	0.25	0.16
O	8	*KLL*	503	0.46	0.69	0.55	0.35	0.17	0.28	0.22	0.15
F	9	*KLL*	647	0.19	0.53	0.46	0.31	0.07	0.21	0.18	0.13
Ne	10	*KLL*	805	0.03	0.36	0.34	0.25	0.01	0.14	0.17	0.10
Na	11	*KLL*	990	...	0.19	0.21	0.16	...	0.08	0.08	0.07
Mg	12	*KLL*	1186	...	0.16	0.20	0.16	...	0.06	0.08	0.07
		LMM	45	29.4	12.3	7.9	4.3	4.7	2.4	1.7	1.00
Al	13	*KLL*	1396	...	0.12	0.17	0.17	...	0.05[a]	0.07[a]	0.07[a]
		LMM	68	24.7	10.9	7.09	3.9	4.0	2.1	1.5	0.90
Si	14	*KLL*	1619	...	0.06	0.12	0.17	...	0.02	0.05	0.05
		LMM	92	16.8	7.9	5.2	2.9	2.7	1.5	1.1	0.67
P	15	*KLL*	1859	...	0.02	0.07	0.09	...	0.01	0.03	0.04
		LMM	120	10.5	5.3	3.6	2.0	1.7	1.04	0.76	0.47
S	16	*KLL*	2117	...	0.01	0.05	0.07	...	0.004	0.02	0.03
		LMM	152	8.8	4.8	3.3	1.9	1.4	0.93	0.70	0.43
Cl	17	*KLL*	2378	...	1.1	26.7	48.2	...	0.001	0.01	0.02
		LMM	181	5.7	3.4	2.4	1.4	0.92	0.66	0.50	0.31
Ar	18	*LMM*	215	4.3	2.9	2.03	1.2	0.69[a]	0.59	0.43	0.28
K	19	*LMM*	252	2.3	1.8	1.3	0.76	0.37	0.34	0.27	0.18
Ca	20	*LMM*	291	2.1	1.3	1.4	0.87	0.35	0.38	0.31	0.20
		MNN	20	114.4	45.1	28.8	15.5	17.9	9.6	8.3	4.1
Sc	21	*LMM*	340	2.2	2.3	1.8	1.1	0.36	0.45	0.37	0.25
		MNN	24	107.8	43.2	27.7	14.9	16.9	9.2	8.0	3.9
Ti	22	*LMM*	418	1.9	2.4	1.9	1.2	0.32	0.47	0.41	0.28
		MNN	27	107.5	43.4	27.9	15.1	16.9	9.2	8.1	4.01
V	23	*LMM*	473	1.6	2.4	1.9	1.3	0.26	0.47	0.42	0.29
		MNN	31	106.6	43.4	27.9	15.1	16.7	9.2	8.1	4.01
Cr	24	*LMM*	529	1.2	2.3	1.9	1.2	0.19	0.44	0.40	0.29
		MNN	36	96.6	39.8	25.6	13.9	15.2	8.5	7.4	3.7
Mn	25	*LMM*	589	0.78	1.9	1.7	1.1	0.13	0.38	0.36	0.27
		MNN	40	81.3	33.9	21.9	11.9	12.8	7.2	6.3	3.2
Fe	26	*LMM*	703	0.51	1.8	1.6	1.1	0.08	0.35	0.35	0.26
		MNN	47	74.7	31.6	20.5	11.2	11.7	6.7	5.9	2.9
Co	27	*LMM*	775	0.29	1.6	1.5	1.1	0.05	0.32	0.32	0.25
		MNN	53	69.0	29.6	19.2	10.5	10.8	6.3	5.6	2.8
Ni	28	*LMM*	848	0.13	1.4	1.4	1.01	0.02	0.28	0.29	0.23
		MNN	61	61.7	27.0	17.6	9.7	9.7	5.7	5.1	2.6
Cu	29	*LMM*	920	0.03	1.2	1.2	0.91	0.01	0.23	0.26	0.21
		MNN	60	53.2	23.6	15.4	8.5	8.4	5.03	4.5	2.3
Zn	30	*LMM*	994	...	0.87	0.94	0.73	...	0.17[a]	0.20[a]	0.17[a]
		MNN	59	37.5	17.2	11.3	6.2	5.9	3.7	3.3	1.7
Ga	31	*LMM*	1070	...	0.64	0.73	0.59	...	0.12	0.16	0.14
		MNN	55	25.6	12.2	8.1	4.5	4.02	2.6	2.3	1.2
Ge	32	*LMM*	1147	...	0.49	0.60	0.50	...	0.09	0.13	0.12
		MNN	23	145.8	58.2	37.2	20.1	22.9	12.4	10.8	5.3
As	33	*LMM*	1228	...	0.41	0.53	0.47	...	0.08	0.11	0.11
		MNN	31	84.9	34.9	22.5	12.2	13.4	7.4	6.5	3.2
Se	34	*LMM*	1315	...	0.29	0.41	0.39	...	0.06	0.09	0.09
		MNN	43	48.1	20.5	13.3	7.3	7.6	4.4	3.8	1.9
Br	35	*LMM*	1396	...	0.18	0.29	0.28	...	0.04	0.06	0.07
		MNN	55	31.3	13.7	8.9	4.9	4.9	2.9	2.6	1.3
Kr	36	*LMM*	1474	...	0.13	0.24	0.24	...	0.03	0.05	0.06
Rb	37	*LMM*	1565	...	0.07	0.15	0.16	...	0.01	0.03	0.04
		MNN	76	17.3	7.9	5.3	2.9	2.7	1.7	1.5	0.77
Sr	38	*LMM*	1649	...	0.07	0.16	0.18	...	0.01	0.03	0.04
		MNN	110	18.2	8.9	5.9	3.3	2.9	1.9	1.7	0.88
Y	39	*LMM*	1746	...	0.06	0.17	0.21	...	0.01	0.04	0.05
		MNN	127	19.6	10.1	6.8	3.8	3.1	2.1	2.0	1.01
Zr	40	*LMM*	1845	...	0.05	0.17	0.23	...	0.01	0.04	0.05

TABLE I (*continued*).

Element	Z	Transition	E_x(eV)	Relative yield, $\rho\sigma N\lambda r \times 10^{20}$				Normalized sensitivity factor			
				1 kV	3 kV	5 kV	10 kV	1 kV	3 kV	5 kV	10 kV
		MNN	147	19.2	10.5	7.1	4.1	3.01	2.2	2.1	1.1
Nb	41	*LMM*	1944	...	0.04	0.16	0.24	...	0.01	0.03	0.06
		MNN	167	18.5	10.7	7.4	4.2	2.9	2.3	2.1	1.1
Mo	42	*LMM*	2044	...	0.02	0.15	0.23	...	0.005	0.03	0.05
		MNN	186	16.6	10.2	7.1	4.1	2.6	2.2	2.1	1.1
Tc	43	*MNN*	249	12.6	9.0	6.5	3.8	2.0[a]	2.0	1.9	1.01
Ru	44	*MNN*	273	1.5	8.7	6.3	3.7	1.8	1.9	1.8	0.99
Rh	45	*MNN*	302	9.7	8.0	5.8	3.5	1.5	1.7	1.7	0.93
Pd	46	*MNN*	330	8.0	7.1	5.3	3.2	1.3	1.5	1.5	0.85
Ag	47	*MNN*	351	6.1	6.0	4.5	2.7	0.95	1.3	1.3	0.73
Cd	48	*MNN*	376	4.3	4.7	3.6	2.3	0.68	1.00	1.05	0.60
In	49	*MNN*	404	3.1	3.8	3.01	1.9	0.48	0.82	0.87	0.50
Sn	50	*MNN*	430	2.07	3.0	2.4	1.5	0.33	0.63	0.69	0.41
Sb	51	*MNN*	454	1.7	2.8	2.3	1.5	0.26	0.60[a]	0.67[a]	0.40[a]
Te	52	*MNN*	483	1.2	2.4	2.0	1.3	0.19	0.51	0.58	0.35
		NOO	31	128.3	52.6	33.9	18.4	14.5	3.7	0.72	0.44
I	53	*MNN*	511	0.78	1.9	1.6	1.1	0.12	0.40	0.47	0.29
		NOO	37	84.1	35.3	22.9	12.5	9.5	2.5	0.48	0.30
Xe	54	*MNN*	532	0.44	1.4	1.2	0.84	0.07	0.29	0.35	0.22
		NOO	41	51.6	22.4	14.6	8.0	5.8	1.6	0.31	0.19
Cs	55	*MNN*	563	0.21	0.91	0.83	0.58	0.03	0.19	0.24	0.16
		NOO	47	17.8	8.0	5.2	2.9	2.01	0.57	0.11	0.07
Ba	56	*MNN*	584	0.17	1.1	1.0	0.71	0.03	0.22	0.29	0.19
		NOO	57	20.2	9.4	6.2	3.4	2.3	0.66	0.13	0.08
La	57	*MNN*	625	0.13	1.2	1.2	0.88	0.02	0.26	0.35	0.23
		NOO	78	42.9	20.3	13.5	7.5	4.8	1.4	0.29	0.18
Ce	58	*MNN*	661	0.07	1.2	1.2	0.87	0.01	0.25	0.34	0.23
		NOO	82	38.5	18.8	12.5	7.0	4.3	1.3	0.27	0.17
Pr	59	*MNN*	699	0.03	1.1	1.1	0.83	0.004	0.22	0.32	0.22
		NOO	87	38.1	18.7	12.5	7.0	4.3	1.3	0.26	0.17
Nd	60	*MNN*	730	0.004	0.96	1.02	0.79	0.0007	0.21	0.30	0.21
		NOO	91	37.0	18.4	12.3	6.9	4.2	1.3	0.26	0.17
Pm	61	*MNN*						...	0.19	0.28	0.20
		NOO						3.9	1.3	0.25	0.16
Sm	62	*MNN*	814	...	0.80	0.91	0.73	...	0.17	0.26	0.19
		NOO	100	33.9	17.4	11.7	6.6	3.8	1.2	0.25	0.16
Eu	63	*MNN*	858	...	0.60	0.70	0.58	...	0.13	0.20	0.15
		NOO	109	27.6	14.3	9.6	5.4	3.1	1.01	0.20	0.13
Gd	64	*MNN*	895	...	0.65	0.79	0.67	...	0.14	0.23	0.18
		NOO	138	34.6	18.3	12.4	7.0	3.9	1.3	0.26	0.17
Tb	65	*MNN*	1073	...	0.65	0.82	0.71	...	0.14	0.24	0.19
		NOO	146	34.0	18.3	12.4	7.01	3.8	1.3	0.26	0.17
Dy	66	*MNN*	1126	...	0.58	0.76	0.67	...	0.12	0.22	0.18
		NOO	151	32.2	17.5	11.9	6.8	3.6	1.2	0.25	0.16
Ho	67	*MNN*	1175	...	0.52	0.71	0.65	...	0.11	0.21	0.17
		NOO	157	30.7	17.1	11.7	6.6	3.5	1.2	0.25	0.16
Er	68	*MNN*	1393	...	0.50	0.71	0.66	...	0.11	0.21	0.18
		NOO	163	17.6	9.9	6.8	3.9	2.0	0.71	0.14	0.09
Tm	69	*MNN*	1449	...	0.45	0.67	0.64	...	0.10	0.19	0.17
		NOO	166	26.5	15.5	10.7	6.1	3.0	1.1	0.23	0.15
Yb	70	*MNN*	1514	...	0.38	0.59	0.58	...	0.08	0.17	0.15
		NOO	170	14.8	8.7	6.02	3.5	1.7	0.62	0.13	0.09
Lu	71	*MNN*	1573	...	0.35	0.58	0.59	...	0.08	0.17	0.16
		NOO	177	14.4	8.7	6.1	3.5	1.6	0.62	0.13	0.08
Hf	72	*MNN*	1624	...	0.35	0.62	0.64	...	0.07	0.18	0.17
		NOO	185	14.3	9.1	6.4	3.7	1.6	0.65	0.14	0.09
Ta	73	*MNN*	1680	...	0.33	0.62	0.67	...	0.07	0.18	0.18
		NOO	179	13.7	9.1	6.4	3.7	1.5	0.64	0.14	0.09
W	74	*MNN*	1736	...	0.29	0.60	0.67	...	0.06	0.17	0.18
		NOO	179	12.7	8.8	6.3	3.7	1.4	0.63	0.13	0.09
Re	75	*MNN*	1799	...	0.26	0.57	0.66	...	0.05	0.17	0.18
		NOO	176	11.6	8.4	6.02	3.5	1.3	0.60	0.13	0.09
Os	76	*MNN*	1850	...	0.22	0.53	0.64	...	0.05	0.15	0.17
		NOO	170	9.5	7.4	5.4	3.2	1.07	0.52	0.11	0.08

TABLE I (*continued*).

Element	Z	Transition	E_x(eV)	Relative yield, $\rho\sigma N\lambda r \times 10^{20}$				Normalized sensitivity factor			
				1 kV	3 kV	5 kV	10 kV	1 kV	3 kV	5 kV	10 kV
Ir	77	*MNN*	1908	...	0.18	0.48	0.60	...	0.04	0.14	0.16
		NOO	171	8.8	7.1	5.2	3.1	1.0	0.50	0.11	0.07
Pt	78	*MNN*	1967	...	0.14	0.42	0.54	...	0.03	0.12	0.14
		NOO	168	7.4	6.2	4.6	2.8	0.83	0.44	0.10	0.07
Au	79	*MNN*	2024	...	0.10	0.35	0.48	...	0.02	0.10	0.13
		NOO	239	7.1	6.3	4.7	2.9	0.80[a]	0.45[a]	0.10[a]	0.07[a]
Hg	80	*MNN*	2078	...	0.07	0.27	0.38	...	0.01	0.08	0.10
		NOO	241	5.0	4.8	3.7	2.2	0.56	0.34	0.08	0.05
Tl	81	*MNN*	2134	...	0.04	0.22	0.32	...	0.01	0.06	0.09
		NOO	244	3.8	4.0	3.03	1.9	0.43	0.28	0.06	0.05
Pb	82	*MNN*	2186	...	0.03	0.18	0.29	...	0.01	0.05	0.08
		NOO	249	3.1	3.5	2.7	1.7	0.35	0.25	0.06	0.04
Bi	83	*MNN*	2243	...	0.02	0.15	0.25	...	0.004	0.04	0.07
		NOO	249	2.3	2.9	2.3	1.4	0.26	0.21	0.05	0.03

[a] Normalization points.

occurring at energies less than 200 eV because of the increased yield due to the excitation by secondaries.

IV. USE OF SENSITIVITY FACTORS WITH DIFFERENTIATED SPECTRA

Table I also lists the values of Auger sensitivity factors for primary electron beams of 1, 3, 5, and 10 kV for the major *KLL*, *LMM*, *MNN*, and *NOO* transitions normalized to sensitivity factors from the *Handbook of Auger Electron Spectroscopy*.[3] These yields can be used for quantitative information if the Auger data are collected with differentiated signal. With this method, the Auger current is assumed to be proportional to the peak-to-peak height. The values of $\rho\sigma N\lambda r$ were normalized to the *Handbook* value of the aluminum sensitivity factor for the *KLL* transitions, to the zinc value for the *LMM* transitions, and to the antimony value for the *MNN* transitions at the respective primary voltages. All of the *Handbook* data are normalized to the silver *MNN* peak generated with a 3 kV primary beam; this procedure was not used because the first principles method assumes that all Auger peaks are of the same general shape and normalizing each transition group to an element in that group is an attempt to account for peak shape changes that occur from transition group to transition group. Normalization for each respective primary voltage is done within each transition group to reduce any error that may be inherent in the cross section values. Aluminum, zinc, and antimony were chosen for the normalization elements because their *Handbook* spectra were relatively contamination free, they were near the center of their transition series, and they were surrounded by elements which also had fairly contamination-free spectra in the *Handbook*. The normalization to these elements, therefore, assumes that their relative yields in the *Handbook* are correct.

The normalization point for the 1 kV data was based upon the shape of the ionization cross section curve (see Fig. 1). The values for the 1 kV yield for carbon, argon, and technetium were extrapolated from 3 and 5 kV data to be 1.34, 0.69, and 1.98; these values were used as the normalization points for *KLL*, *LMM*, and *MNN* transitions, respectively. The value for the *NOO* sensitivity factor for the gold transitions with a 3 and 5 kV electron beam were obtained by measuring the peak-to-peak height in the *Handbook*. The values for the 1 and 10 kV Au_{NOO} were extrapolated by using the 3 and 5 kV values and the shape of the cross section curve.

These values should not be used for quantitative calculations if the energy of the Auger peak is below 200 eV for the two reasons outlined earlier: a lower multiplier gain at lower energies and secondaries from the bulk contributing to the Auger yield.

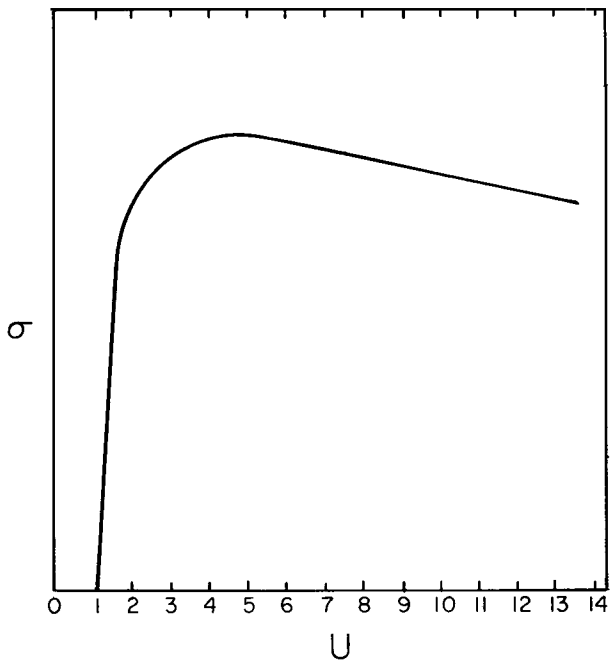

FIG. 1. Plot of ionization cross section (relative intensity units) vs reduced energy.

V. USE OF SENSITIVITY FACTORS OR CALCULATED YIELDS TO DETERMINE ATOMIC PERCENT CONCENTRATION

As outlined in the *Handbook*, relative sensitivity factors (i.e., relative yields) can be used to calculate the concentration of elements above atomic number 2. The atomic concentration can be expressed as:

$$X_i = \frac{Y_i/S_i d_i}{\sum_\alpha Y_\alpha/S_\alpha d_\alpha}, \tag{3}$$

where X_i is the atomic concentration of element i, Y_i the peak-to-peak intensity or the area under the undifferentiated peak, S_i the relative sensitivity of element i, and d_i is a scale factor defined by

$$d_i = L_i i_p, \tag{4}$$

where L_i is the lock-in amplifier sensitivity and i_p is the primary beam current. It is assumed the modulation voltage is held constant for those spectra collected in the differentiated mode.

VI. CONCLUSIONS

The relative Auger yield was calculated with a method which combined the effects of the ionization cross section, the atomic density, the electron escape depth, the backscattering factor and the Auger transition probability. The relative yields are presented along with values which were normalized to primary voltage and transition specific sensitivity factors in the *Handbook of Auger Electron Spectroscopy*. The relative yields can be used for quantitation if the spectra were collected with pulse-counting electronics while the normalized sensitivity factors can be used if the spectra were collected through a lock-in amplifier. The normalization attempts to account for the different derivative peak shapes; the as-calculated yields do not have a peak shape variable. An examination of the technique showed the importance of atomic density fluctuations and sample roughness on final quantitative accuracy. The hazards of using calculated values for quantitation of transitions below 200 eV in energy were found to be twofold: a lower multiplier gain at lower energies (for spectra collected in the derivative mode) and secondary electrons from the bulk which cause increased yields at low energy values.

[1]S. Mroczkowski and D. Lichtman, Surf. Sci. **127**, 119 (1983).
[2]S. Mroczkowski and D. Lichtman, Surf. Sci. **131**, 159 (1983).
[3]P. W. Palmberg, G. E. Riach, R. E. Weber, and N. C. MacDonald, *Handbook of Auger Electron Spectroscopy* (Physical Electronics, Edina, MN, 1972).
[4]A. R. DuCharme and R. L. Gerlach, J. Vac. Sci. Technol. **11**, 281 (1974).
[5]M. P. Seah and W. A. Dench, Surf. Interface Anal. **1**, 2 (1979).
[6]W. Reuter, in *Proceedings of the 6th International Conference on X-Ray Optics and Microanalysis*, edited by G. Shinoda, K. Kohra, and T. Ichinokawa (University of Tokyo, Japan, 1972), 121.
[7]E. H. S. Burhop, *The Auger Effect and Other Radiationless Transitions* (Cambridge University, London, 1952), p. 48.
[8]P. Holloway, J. Electron Spectrosc. Relat. Phenom. **7**, 215 (1975).
[9]C. C. Chang, in *Characterization of Solid Surfaces*, edited by P. F. Kane and G. B. Larrabee (Plenum, New York, 1974), p. 509.
[10]G. E. McGuire, *Auger Electron Spectroscopy Reference Manual* (Plenum, New York, 1979).
[11]D. M. Smith and T. E. Gallon, J. Phys. **7**, 151 (1974).
[12]C. J. Powell, in *Proceedings of the Seventh International Vacuum Congress and Third International Congress on Solid Surfaces* (R. Dobrozemsky, Vienna, 1977), p. 2319.
[13]H. E. Bishop and J. C. Rivière, J. Appl. Phys. **40**, 1740 (1969).
[14]R. L. Gerlach and A. R. DuCharme, Surf. Sci. **32**, 329 (1972).
[15]C. J. Powell, Rev. Mod. Phys. **48**, 33 (1976).